International Journal of Mathematics and Physical Sciences Research ISSN 2348-5736 (Online)
Vol. 7, Issue 1, pp: (75-83), Month: April 2019 - September 2019, Available at: www.researchpublish.com

Influence of Surfactants on the Morphology and Stoichiometry of Hydrothermally Synthesised Cu_2ZnSnS_4 (CZTS) thin films for Solar cell Application

Kasim Ibrahim Mohammed[1,4,*], Kasim Uthman Isah[1], Uno Esang Uno[1], Abdullahi Mann[2], Nafarizal Nayan[3]

[1]Department of Physics, Federal University of Technology, Minna, NIGERIA

[2]Department of Chemistry, Federal University of Technology, Minna, NIGERIA

[3]Microelectronics and Nanotechnology Shamsuddin Research Centre (MiNT-SRC), Institute for Integrated Engineering (I^2E), Universiti Tun Hussein Onn Malaysia, 86400 Parit Raja, Johor, MALAYSIA

[4]Department of Physical Sciences, Niger State Polytechnic, Zungeru, NIGERIA

[*]Corresponding, kasimzabbo@yahoo.com

Abstract: **Cu_2ZnSnS_4 (CZTS) films were synthesised using hydrothermal method, while varying the surfactants as Polyacrylic acid, polyvinylpyrrolidon, polyethylene glycol and polyvinyl alcohol. The XRD reveal characteristic peaks of CZTS (112) and (220) for the sample synthesised using polyacrilic acid and in addition, numerous other peaks were observed for the remaining samples synthesised. The average crystallite sizes range between 8.76 and 19 nm. Raman spectra of the films reveal CZTS peaks of 338, 351 and 252 $cm^{-1}$for samples synthesised using polyacrilic acid precursor while ZnS, SnS, Cu_3SnS_3, Cu_3SnS_4, Sn_2S_3 secondary and ternary phases were observed for other surfactants in addition to the 338 CZTS peak. SEM image show spherical nanoparticles and agglomerated nanosphere-like shapes. The Cu: Zn: Sn: S atom ratios were close to stoichiometry for polyacrylic acid and polyvinylpyrrolidon surfactants. There is significant deviation from stoichiometry for the other surfactants. The average surface roughness was between 800 and 2000 nm. The bandgap energy obtained from the optical characterisation varied between 1.51 eV and 1.56 eV.**

Keywords: **Cu_2ZnSnS_4, Hydrothermal, Surfactant, Thin film, Reaction Duration, Morphology, Stoichiometry.**

I. INTRODUCTION

Cu_2ZnSnS_4 (CZTS), with an optimal direct band-gap of 1.5 eV and a large absorption coefficient of over 10^4 cm^{-1} [1], is one of the most promising materials as the absorber layers of thin-film solar cells. Its optical properties and crystal structure are similar to the chalcopyrite type semiconductor of $CuIn_{1-x}Ga_xSe_2$ (CIGS), one of the most successful thin-film photovoltaic materials for commercial use. However, unlike CIGS containing the expensive and toxic constituent elements such as Ga, In and Se, CZTS is composed of the earth-abundant elements: copper, zinc, tin and sulphur. All of them are nontoxic, so CZTS is considered as a suitable replacement for CIGS in its thin-film solar cells, to obtain the CZTS thin-film solar cells. CZTS thin film solar cell have achieved the power conversion efficiency of 10.1%, using the $Cu_2ZnSn(Se,S)_4$ kesterite absorber [3].

In the last two decades, various vacuum methods have been investigated for the deposition of CZTS thin films, such as atom beam sputtering method [1], RF magnetron sputtering deposition [4], pulsed laser deposition method [6] and thermal evaporation of elements method [7], but all of the methods impose an additional cost on the technology. Thus, non-vacuum alternative techniques, such as electrochemical deposition [8], spray pyrolysis deposition [10], the sol–gel method [11], nanocrystals''ink'' printing technology [7] and hydrothermal synthesis of CZTS nanoparticles followed by doctor blading deposition have been rapidly developing. Among these methods, hydrothermal synthesis technology has drawn much attention, because it is one of the facile non-vacuum methods that does not require any expensive precursors or equipment and can be readily adopted for industrial production processes. It possesses remarkable reliability and selectivity as well as high efficiency at low temperature.

Polymer based surfactants such as polyacrylic acid (PAA), polyethylene glycol (PEG), polyvinylpyrrolidone (PVP) and polyvinyl alcohol (PVA) have been widely employed in hydrothermal and solvothermal methods for the preparation of inorganic nanomaterial oxides and sulfides such as titanium oxides, copper sulfides and zinc sulfides.16-19 It is generally assumed that the polymers act as structure-directing agents or soft templates, which can control the morphology and size of the particles formed in the hydrothermal or solvothermal reaction through influencing their nucleation and growth process. Suitable polymers have been used in the solvothermal method to synthesize pure phase CZTS nanoparticles as well as to tune the morphology and size of the particles.

This work reports the hydrothermal approach of synthesising CZTS nanoparticles using PAA, PEG, PVP and PVA as the surfactant in the aqueous precursor solutions. The influence of the various surfactants on the synthesis of CZTS was investigated and the properties of the CZTS nanoparticles including the crystal structure, morphology and elemental composition were determined using XRD, RAMAN spec, SEM EDX, AFM, UV-Vis spec, FTIR and four point probe.

II. METHODOLOGY

All the chemicals used were purchased from Sigma Aldrich unless otherwise stated. 0.2 mmol of $CuCl_2.2H_2O$, 0.1 mmol of $ZnCl_2$, 0.1 mmol of $SnCl_4.5H_2O$, 0.5 mmol of C_2H_5NS and 1.0 g of PEG, PVP, PVA and PAA were in each case dissolved in 36 ml of deionised water under magnetic stirring. The resulting solutions were transferred to a Teflon-lined stainless steel autoclave of 45 ml capacity, which were then in each case sealed and maintained at 150 °C each for 24 h. After that, the autoclave in each case was allowed to cool to room temperature naturally.

The resulting black precipitate of each sample was centrifuged and washed with deionised water, absolute ethanol and acetone several times. Finally, the products were vacuum-dried at 80 °C for 5 hours. The samples were labelled PEG, PVP, PVA and PAA for samples synthesised using Polyethylene glycol, Polyvinyl pyrrolidone, Polyvinyl alcohol and Polyacrylic acid respectively.

The dried powders obtained from as-synthesized CZTS nanocrystals were prepared for thin film deposition by dispersing the CZTS powder (10%, w/w) in mixture of terpineol and triton X-100 (85%:5%, w/w). The slurry was then subjected to rigorous magnetic stirring for 48 hours.

Thin films were then prepared by depositing the CZTS slurry on fluorine doped tin oxide (FTO) coated soda lime glass (FTO/SLG) substrate by doctor-blading. The thin films were then annealed in a graphite box containing sulphur powder at 550 °C for 30 min in a rapid thermal annealing processing (RTP) system with a heating rate of 10 °C/min. A static annealing atmosphere of 0.3 atm argon was supplied in the RTP furnace.

Before deposition, the substrate was prewashed thoroughly with deionised water, acetone, and ethanol in sequence under sonication for 10 min each followed by being blow-dried with nitrogen gas.

The crystallographic structure and phase analysis of the synthesized thin film samples were done by X-ray diffraction (XRD, PANanalytical XPert Pro Multi-Purpose Diffractometer (MPD), CuKα, λ = 0.154056 nm). The Raman spectra of the samples were recorded with a Raman spectrometer (Xplora Plus, Horiba Scientific Raman microscope) with a 785 nm excitation laser to distinguish possible secondary phases in the films. The morphology and the elemental analysis of the samples were characterised by scanning electron microscopy (SEM, JEOL 7600F) at an acceleration voltage of 20.0 kV combined with an energy dispersive X-ray spectroscopy (EDS). Surface roughness and topology measured using (Hitachi 5100N) atomic force microscope (AFM). Ultraviolet-visible (UV-vis) absorption spectrum of the samples was measured

at room temperature using a Shimadzu UV-1800 spectrophotometer. The Infra-red spectra of the samples were measured using Perkin-Elmer, G-FTIR spectrometer. The thickness of the films was measured using Alpha step Q 7083319 surface profiler, while the electrical resistivity measurement of the thin film samples was done using (signatone PRO 4, LUCAS LABS 2400) four point probe

III. RESULTS AND DISCUSSION

The XRD patterns of the CZTS thin film samples obtained using different surfactant are shown in Fig. 1 below.

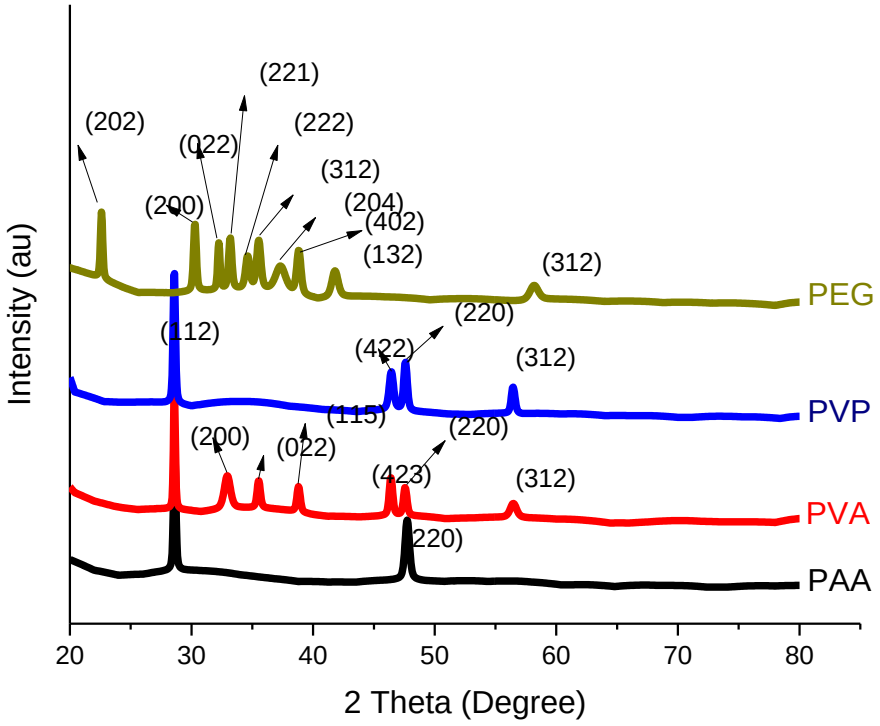

Fig. 1.0 XRD patterns for different surfactants in CZTS thin films

Variation in the surfactant plays a vital role in the structure of the thin film material. Three of the films show preferential orientation along (112) plane (that is, the one synthesised using PAA, PVA and PVP). Crystallite size of the films also varies with variation in surfactants. From the XRD peaks, the 2Θ values for 28.59^o corresponding to (112) plane for sample PAA, 28.32^o also corresponding to (112) plane for sample PVA, then 28.71 also corresponding to (112) plane for PVP and 22.81^o also corresponding to (202) plane for PEG. The XRD pattern of the samples synthesised using PEG, PVP and PVA surfactants shows that impurities Cu_2S and SnO_2 coexist within the CZTS product. Also, PVP and PVA samples shows better crystallinity as compared to PEG as evident with many peaks observed in the XRD spectrum of the CZTS sample synthesised using PEG surfactant. The PAA sample exhibits only the (112) and (220) peaks which are kesterite CZTS (ICSD 98-018-4358).

The crystallite sizes of the samples were calculated using Debye Scherer's formula as shown in table 1.0 below;

$$D = \frac{\kappa\lambda}{\beta\cos\theta} = \frac{0.94\lambda}{\beta\cos\theta}$$

Where β is full width at half maximum (FWHM), θ is diffraction angle, *k* is a constant of approximate 0.94 Shape factor and λ is wavelength of the X-rays (1.5406 Å or 0.15406 nm) and D is crystallite size respectively.

TABLE I: FWHM AND CRYSTALLITE SIZE OF CZTS THIN FILM SAMPLES SYNTHESISED AT DIFFERENT REACTION TEMPERATURES

Sample Name	FWHM (^{o})	Average Crystallite size (nm)	2Ɵ (^{o})	d-spacing (Å)	h k l	Lattice parameters a (Å)
PEG	14.28	16.00	22.81	3.89585	202	10.92
	27.55	14.28	30.59	2.91950	311	
	39.36	11.01	31.34	2.85240	022	
	35.42	19.00	32.32	2.76749	221	
	27.55	15.90	34.11	2.62662	222	
	35.42	12.32	35.82	2.50422	312	
	39.36	11.11	38.71	2.32436	204	
	43.30	14.23	40.93	2.20315	402	
	31.49	17.23	43.99	2.05632	132	
	47.23	16.23	57.73	1.59571	530	
PVP	14.29	15.00	28.71	3.10889	112	11.03
	42.23	14.29	47.09	1.92978	422	
	47.23	09.45	48.76	1.86757	024	
	39.36	11.56	58.36	1.58109	315	
PVA	14.27	10.00	28.32	3.14850	112	12.60
	47.23	14.30	33.41	2.68001	402	
	31.49	09.46	34.09	2.67909	022	
	27.55	08.76	35.17	2.55000	115	
	35.42	11.43	46.53	1.95033	423	
	23.62	15.98	47.77	1.94103	024	
	39.36	17.39	57.45	1.60286	043	
PAA	14.30	19.00	28.59	3.12209	112	5.43
	34.95	14.00	47.70	1.90657	024	

The lattice parameter ‘a’ for PAA sample was close to the value of 5.4270 Å for tetragonal unit cell kesterite CZTS. Other samples had values of 10.92 Å, 11.03 Å, and 12.6 Å which which are higher values due to larger d-spacing values. The crystal interplanar spacing of 3.12 Å, can be ascribed to the (112) plane of kesterite phase CZTS. The crystallite sizes range between 8.76 and 19.00 nm, the PAA sample had the highest crystallite size and the PVA sample had the least size of 8.76 nm.

Definitive structural analysis and electronic excitation states of the lattice that provide information on possible secondary phases in a material is provided by Raman Spectroscopy.

Raman scattering gives a more definitive structure analysis [3]. The Raman spectra for sample PAA clearly show the peaks at 252 cm^{-1}, 338 cm^{-1} and 351 cm^{-1} which are CZTS kesterite peaks [4]. For surfactants PEG, PVP and PVA, in addition to the 338 cm^{-1} CZTS peak, the 215 cm^{-1}(SnS), 265 cm^{-1}(ZnS), 238 cm^{-1}(Cu_3SnS_3), 285 cm^{-1}(Cu_3SnS_4) and 325 cm^{-1}(Sn_2S_3) peaks were observed. These peaks are usually attributed to secondary phases and impurities [8]. These impurities may be due to the weaker chelating role played by these polymer surfactants (PEG, PVP and PVA) with the metal cations. They may also have weaker adsorption on the primary nuclei surface thus their failure to effectively control the growth rate of CZTS.

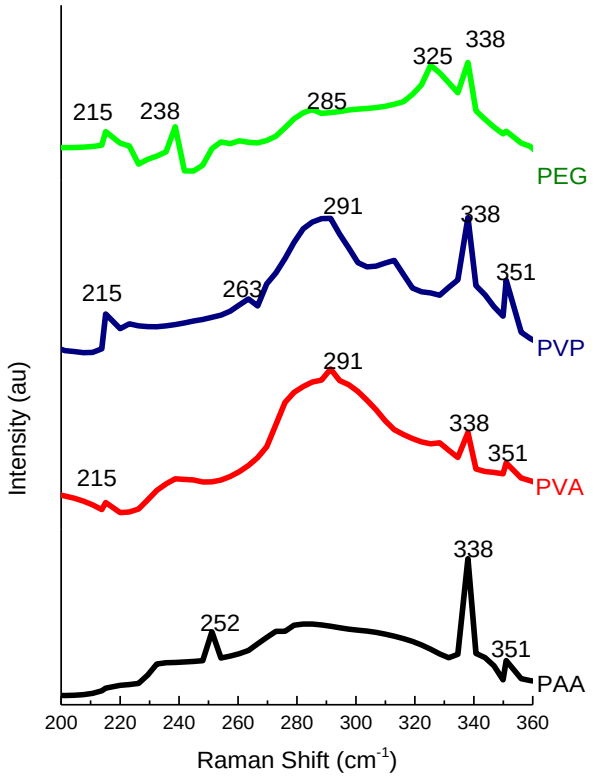

Fig. 2 Raman spectra for CZTS samples synthesised using different surfactants

SEM images of the synthesised CZTS thin films using PEG, PVP and PVA surfactants shows agglomeration of small crystals with no significant morphological differences as shown in Fig. 3 below

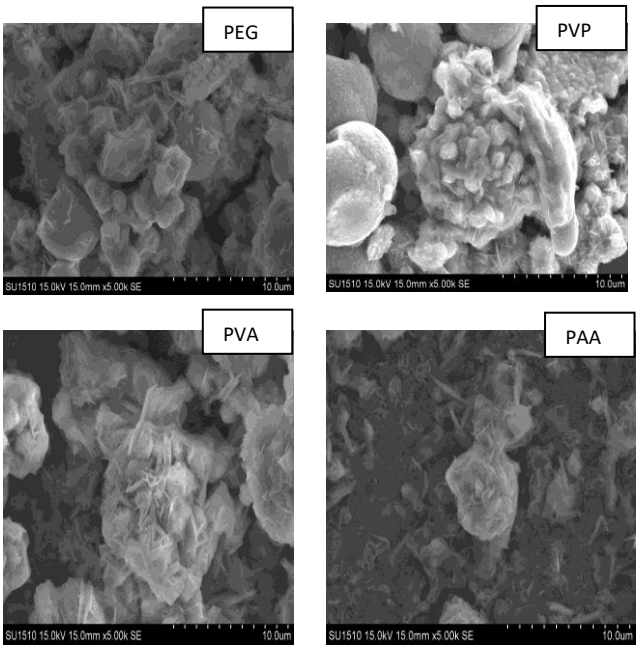

Fig. 3 SEM images for CZTS samples synthesised using different surfactants

The images illustrates that all the films were composed of several intersectional spherical shaped particle. The PVA and PVP films tend to have closely parked spheres. The EDS data shows that the film composed of Cu, Zn, Sn and S as shown in Table II below.

TABLE II: EDS DATA FOR CZTS THIN FILM SYNTHESISED USING DIFFERENT SURFACTANTS

Sample	Cu (at.%)	Zn (at.%)	Sn (at.%)	S (at.%)	$\frac{Cu}{Zn+Sn}$	$\frac{Zn}{Sn}$	Cu/Zn/Sn/S
PEG	22.3	7.6	19.7	48.8	0.82	0.39	2.93:1.00:2.59:6.42
PVP	22.7	11.9	15.1	47.9	0.84	0.79	1.91:1.00:1.27:4.03
PVA	22.4	9.1	16.7	48.1	0.78	0.55	2.46:1.00:1.84:5.29
PAA	23.1	11.8	13.5	48.9	0.91	0.87	1.97:1.00:1.35:4.17

From Table II above, the atomic percentage of Cu and S did not show significant changes as for sample synthesized using PEG and PVA. The ideal CZTS stoichiometric ratio entails Cu/(Zn + Sn) and Zn/Sn be equals 1, while the ideal the ideal Cu: Zn: Sn: S stoichiometric value is 2:1:1:4. The PAA and PVP samples reveal near ideal compositional ratio for Cu/Zn + Sn of 0.91 and 0.84, Zn/Sn ratio of 0.87 and 0.79 respectively, these values though shows they are both Cu poor and Zn poor. Cu/(Zn + Sn) atomic ratio of near 0.85 have however been reported to show good optoelectronic properties and best device efficiency [6]. The slightly Sn rich and Zn poor composition for PAA and PVP may be ascribed to the reactivities of the different metal precursor [12]. The Cu:Zn:Sn:S ratios of 1.97:1.00:1.35:4.17 and 1.91:1.00:1.27:4.03 for the PAA and PVP samples respectively were close to ideal stoichiometric value of 2:1:1:4. Samples PEG and PVA however show significant deviation from ideal CZTS composition exhibiting very high Cu and S content. These samples show significant decrease in the Zn/Sn ratio. The Zn/Sn ratios shows the samples are Sn rich and Zn poor, with PEG and PVA showing significantly high Sn content compared to Zn.

Fig. 4 below show the AFM images of CZTS thin film samples synthesised at different hydrothermal reaction temperatures. AFM provides 3-Dimensional and 2-Dimensional profiles of the sample surface on a nanoscale. In this work, it is observed from the figure that the morphology of these films was uniform surface with clear grain boundaries and growth of crystal.

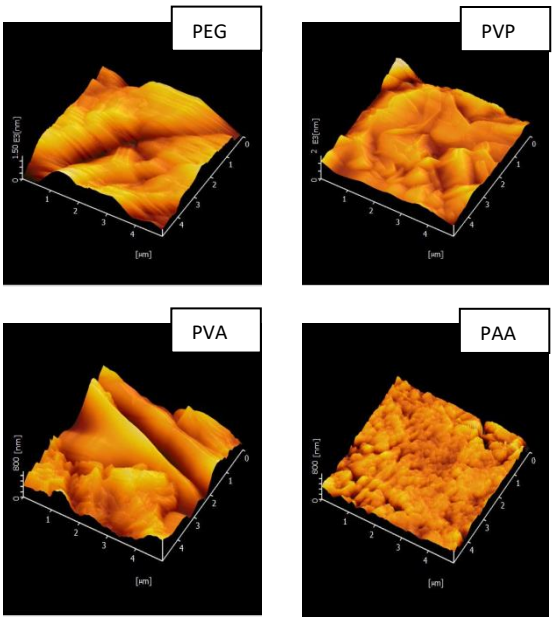

Fig. 4 AFM image for CZTS thin film samples synthesised using different surfactants

The AFM 3D surface visualization of the CZTS thin film shows granular variations. The values of roughness shows that samples PEG (1.5 x 10^3 nm), PVP (2.0 x 10^3 nm), PVA (0.8 x 10^3 nm) and PAA (0.8 x 10^3 nm) these values show that the surfaces was quite smooth. A relatively smooth surface allows good physical contact with the subsequent layer and avoids the shorting that may arise due to uneven surface topography.

For a direct band gap material the absorption coefficient satisfy the relation $(\alpha h\nu)^2 = A(h\nu - Eg)$, where α, ν, Eg and A are the absorption coefficient, light frequency, band gap energy and a constant respectively. The direct band gap Eg calculated by extrapolating the linear portion of the curves of $(\alpha h\nu)^2$ vs. (hν) gives values of Eg as shown in Table III and Fig. 5 below. The bandgap and also the absorption coefficient values are in good agreement with the reported values in literature [2]. These values are close to optimal bandgap and absorption coefficient of 1.45 eV and 10^4 cm^{-1} respectively for absorber layer application in solar cells.

TABLE III: BAND GAP, ABSORPTION COEFFICIENT, SURFACE ROUGHNESS AND ELECTRICAL RESISTIVITY OF CZTS THIN FILMS SYNTHESIZED USING DIFFERENT SURFACTANTS

S/N	Sample	Absorption coefficient (A) (cm^{-1})	Band gap (Eg) (eV)	Surface Roughness (nm)	Resistivity (Ωcm)
1	PAA	1.37 X 10^4	1.55	0.8 x 10^3	4.02 x 10^{-2}
2	PEG	1.39 X 10^4	1.51	1.5 x 10^3	1.23 x 10^{-2}
3	PVP	1.34 X 10^4	1.56	2.0 x 10^3	2.02 x 10^{-2}
4	PVA	1.38 X 10^4	1.52	0.8 x 10^3	4.02 x 10^{-2}

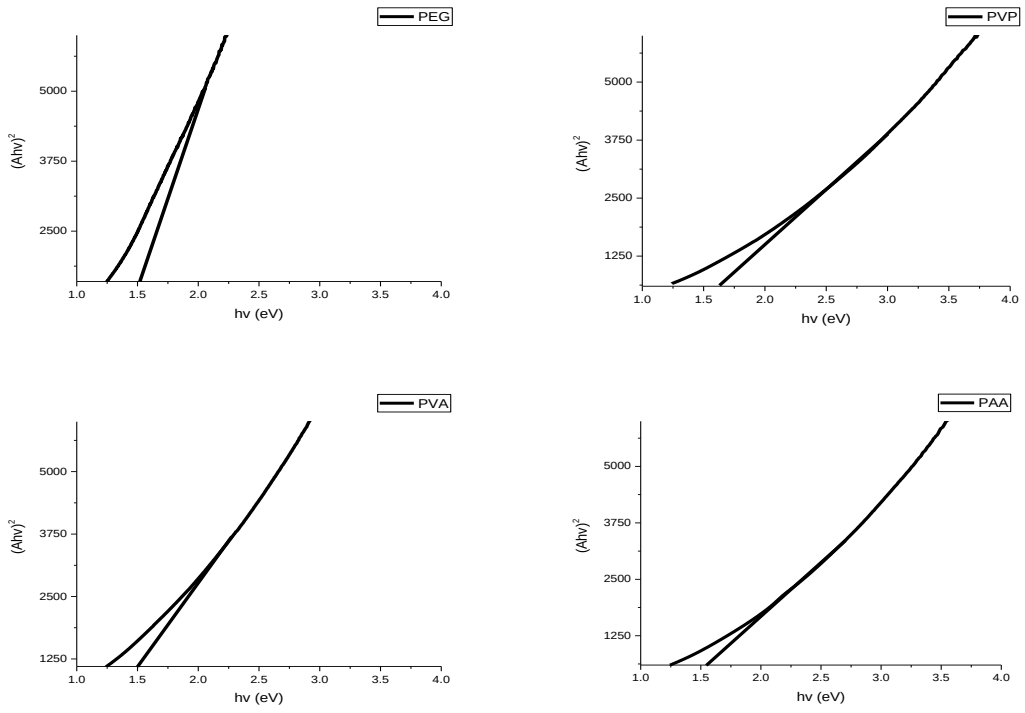

Fig. 5 Energy band gap spectral analyses for CZTS thin film samples synthesised using different surfactants

As complementary characterizations, the FTIR analysis was carried out for the samples. FTIR response for the four samples is shown in fig. 6 below. It reveals the presence of various bands at 630, 1129, and 1451 cm^{-1}. The peak at 630 is usually attributed to metal–sulphur complexes. Bands around 900–1600 cm^{-1} are due to oxygen stretching and banding frequency. Weak additional bands at 950 and 884 cm^{-1} are attributed to the resonance interaction between vibrational modes of sulphide ions in the crystal.

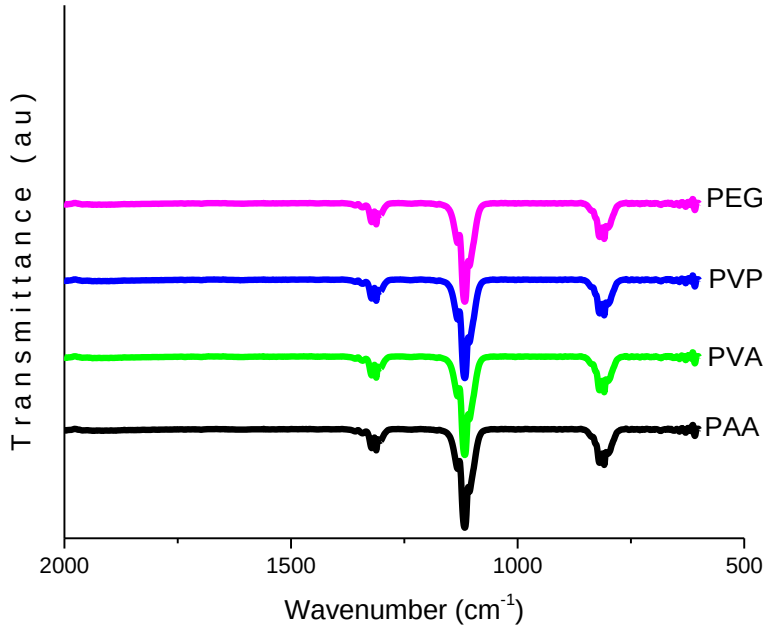

Fig. 6 FTIR spectra for CZTS thin film samples synthesised using different surfactants

The thickness of a film has a critical role in the properties of thin films. In this present work, it is observed that irrespective of the variation in hydrothermal reaction temperature the film thickness was approximately 3.6 x 10^{-1}µm.

The resistivity values for PAA and PVA recorded higher values as compared to PEG and PVP samples. All the resistivity values obtained exhibited the p-type semiconductor material property of 10^{-2} Ωm as shown in Table III above.

IV. CONCLUSION

This research work systematically examined the influence of various surfactants on the formation of CZTS nanocrystals using the hydrothermal method. Kesterite CZTS film was obtained using polyacrylic acid surfactant with no secondary phase, ZnS, SnS, Cu_3SnS_3, Cu_2SnS_4, and Sn_2S_3 secondary and ternary phases were observed for surfactants PEG, PVP and PVA. The Cu:Zn:Sn:S ratios of 1.97:1.00:1.35:4.17 and 1.91:1.00:1.27:4.03 for the PAA and PVP samples respectively were close to ideal stoichiometric, there is however significant stoichiometric deviation for the samples PEG and PVA, exhibiting significant Zn deficiency. The optical band gap of the sample samples was between 1.51 and 1.56 eV.

For pure phase CZTS material that has the capacity for being used as best solar cell absorber material, the PAA surfactant should be used in the synthesis. It was revealed that the surfactant used in the precursor solution during hydrothermal reaction process influences both the compositional and stoichiometry of the crystal structure of the synthesised samples

REFERENCES

[1] Ahmet, T., Abdullah, G., Muharram, Z. Z. & Ferhat, A. (2018). Structure, morphology and optical properties of the vacuum-free processed CZTS thin film absorbers. *Materials Research Express*, (59): 102-104

[2] Chalapathi, U., Uthanna, S. & Raja, S. (2015). Growth of Cu_2ZnSnS_4 thin films by a two stage process-Effect of incorporating of sulfur at the precursor stage. *Solar Energy Materials and Solar Cells*, (132): 476-484

[3] Das, S., Sa, K., Mahakul, P. C., Raiguru, J., Alam, I., Subramanyam, B. V. R. S and Mahanandia, P (2018), Synthesis of quaternary chalcogenide CZTS nanoparticles by a hydrothermal route, *IOP Conf. Series: Materials Science and Engineering* (338): 012062

[4] Fernandes, M., Cao, L., Zhang, B. L. & Jiang, J. C. (2009). One step deposition of CZTS thin films for solar cells. *Solar Energy Materials and Solar Cells*, (117): 81-86

[5] Ito, K. (2015). *Copper Zinc Tin Sulfide-Based thin film solar cells*. John Wiley and Sons Ltd. 93-199

[6] Katagiri H., Jimbo K., Maw W. S., Oishi K., Yamazaki M., Araki H., *et al*. (2009). Development of CZTS-based thin film solar cells. *Thin Solid Films* (517):2455 2460

[7] Nagoya, K. V., Pawara, S. M., Shinb, S. W., Moona, J. H. & Kima, P. S. (2010). Electrosynthesis of CZTS films by sulfurization of CZT precursor: effect of soft annealing treatment. *Applied Surface Science*, (238): 74-80

[8] Price, D. B., Mitzi, O., Gunawan, T. k. & Wang, K. (1999). The path towards a high performance solution-processed kesterite CZTS. *Solar Energy Materials and Solar Cells*, (95): 1421-1436

[9] Tiong, T. T., Hreid, T., Will, G., Bell, J., & Wang, H. (2014). Polyacrylic acid assisted synthesis of CU_2ZnSnS_4 by hydrothermal method. *Science of Advanced Materials*, (6): 1467-1474

[10] Wadia, C., Alivisatos, A. P. & Kammen, D. (2009). CZTS-based solar cell from sol-gel spin coating and its characterization. *Evironment Science and Technology*, (43): 2072-2077

[11] Wang, K., Mitzi, D. B., Barkhouse, R. & Aaron, D. (2011). Prospects and performance limitations for Cu-Zn-Sn-S-Se photovoltaic technology. *Philadelvia Transnational Royal Society*, (371): 1-22

[12] Wei A., Yan, Z., Zhao, Y., Zhuang, M. and Liu, J. (2015). Solvothermal synthesis of Cu2ZnSnS4 nanocrystalline thin films for application of solar cells. *International Journal of Hydrogen Energy*, (40); 797-805